

# Chapter 4

## Optical Metamaterials

Kotaro Kajikawa

**Abstract** Optical metamaterials show interesting optical properties originating from their higher-order structures. We can obtain optical media with a wide range of refractive indexes: from negative to positive large values. This allows us to realize special optical functions such as super high resolution microscopy and optical croaking. In future, various useful optical properties will be found or created in optical metamaterials. This chapter deals with the concept of the optical metamaterials and some optical applications.

### 4.1 Introduction

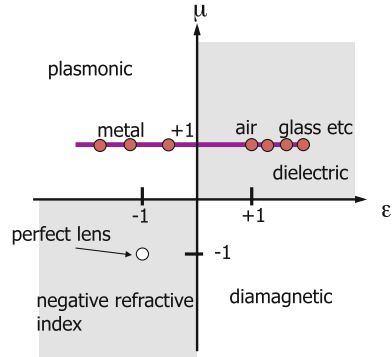
Optical metamaterials [1] show high functionality originating from their higher order structures. Similar things are found in proteins in a biological system that the functionality is due to their higher-order structure. Metamaterials start to be investigated at microwave frequencies. The original concept was that an assembly of electrical circuits is compared to a matter, since the electromagnetic response from the electrical circuits, such as LC resonators, can mimic the response from the matter. In the last decade, this concept is extended to light frequencies. Negative index materials and the optical cloaking technique at optical frequencies are realized, not only because of the development of micro and nano-fabrication techniques but also the development of design for metamaterials. The basic concept to realize the metamaterials is the control of permittivity and permeability by designing the nanostructures. In addition, surface plasmons play an important role to control its permittivity. It is sure that metamaterials will be an important research field as photonic materials in future.

---

K. Kajikawa (✉)

Interdisciplinary Graduate School of Science and Engineering, Tokyo Institute of Technology,  
Nagatsuta, Midori-ku, Yokohama, 226-8502 Japan  
e-mail: kajikawa@ep.titech.ac.jp

**Fig. 4.1** Plots of existing matters and metamaterials in  $\epsilon - \mu$  plain



### 4.2 Metamaterials and Meta-Molecules

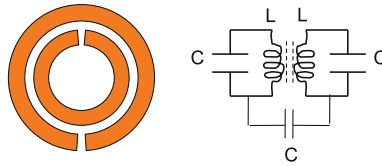
Metallic nanostructures much smaller than the optical wavelength sometimes show interesting optical properties that are not found in existing bulk materials. Most of them are ascribed to surface plasmons that sometimes cause a huge polarizability at their resonance wavelength. Metallic nano-materials allow us to control not only permittivity but also permeability because of the fast response of free electrons in a metal. One of them is negative refractive index. The refractive index  $n$  of a matter is written by

$$n = \pm\sqrt{\epsilon\mu} \tag{4.1}$$

where  $\epsilon$  and  $\mu$  are its permittivity and permeability, respectively. The permeability of an existing material is unity because the magnetic response of a matter is absent at optical frequencies. This is because the magnetism comes from the orbital or spin angular momentum, whose response time is below the frequency range of microwaves. On the other hand, the permittivity of existing materials is ranging from  $-25$  to  $16$ . As a result, the real parts of the refractive indexes of the existing materials are ranging from  $0$  to  $4$  at optical frequency. This is shown in Fig. 4.1, in which existing materials are plotted. They are plotted on the line of  $\mu = 1$ .

The sign of the refractive index is determined by the sign of the permittivity and permeability [1–4]. If both are negative, the refractive index is negative. Such materials are called “left handed materials (LHM)” or “negative index materials (NIM)”. Metamaterials and some kinds of photonic crystals have possibility to be LHM [5]. If we have LHM at optical frequency, incomprehensible phenomena will appear such as negative refraction and super resolution.

An interesting thing is that a medium with negative permeability or permeability of other than unity can be made of existing materials with permeability of unity. As is described above, the magnetism is produced by rotational movement of electrons, which produces angular momentum. Similar effect will appear by the current flow in a circular coil. We can achieve  $\mu \neq 1$  by a current flowing in a resonator shown in



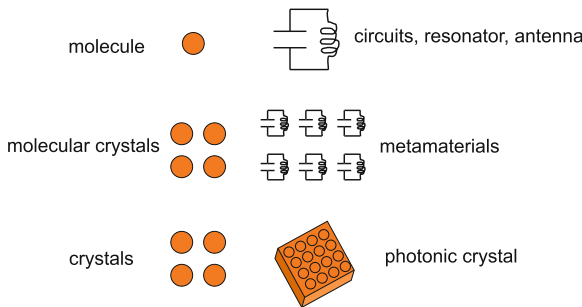
**Fig. 4.2** Split ring resonator and its equivalent circuit

Fig. 4.2, whose size is much smaller than the wavelength of light. Such a resonance structure has a permeability  $\mu$  that is written as

$$\mu(\omega) = 1 - \frac{\omega_{mp}^2 - \omega_{mo}^2}{\omega^2 - \omega_{mo}^2 + i\Gamma_m\omega} \tag{4.2}$$

where  $\omega$  is the frequency,  $\omega_{mp}$  is magnetic plasma frequency,  $\omega_{mo}$  is the magnetic resonance frequency, and  $\Gamma_m$  is the damping constant [6]. If the resonance is strong, the permeability  $\mu$  is ranging from negative to positive. Permittivity also shows similar relation. Therefore we can control the both permittivity and permeability separately by the design of the LC resonance circuit. This is the concept of usual metamaterials. Metamaterials have the refractive index of not only negative values but also a large positive values that the existing materials do not have. Such materials will also show attractive nonlinear optical properties.

Next we consider the similarity between metamaterials and existing matters. The correspondence is summarized in Fig. 4.3. The existing matters can be divided into two categories: one atoms and molecules and the other aggregates and crystals. Atoms and molecules show their own functionality even if interactions between them are absent, namely, they are isolated. This is because their functionality is intrinsic and closed inside the unit. Dye molecules are semiconductor that absorbs light, even if they are isolated in solution. On the other hand, inorganic semiconductors such as silicone show their functionality only in a crystalline form. The isolated atoms do not



**Fig. 4.3** Comparison of existing matters with metamaterials

show the functionality appearing in a crystal. Metamaterials are similar to the atoms and molecules, since it shows optical (electromagnetic) functionality even each unit is separated. Hence, their unit is sometimes called meta-atom or meta-molecules. Metamaterials are an assembly of the meta-atoms or meta-molecules and show the optical properties as an ensemble of the whole units.

Although the metamaterials exhibit their optical functionality of each unit, their aggregates or crystals will also show a new or additional functionality, like molecular aggregates or molecular crystals. An example is that gold bisphere shows a strong red-shifted resonance band, which is not observed in isolated gold nanospheres. As is discussed above, similarity of metamaterials to existing atoms and molecules provides great insight to develop a new class of optical materials.

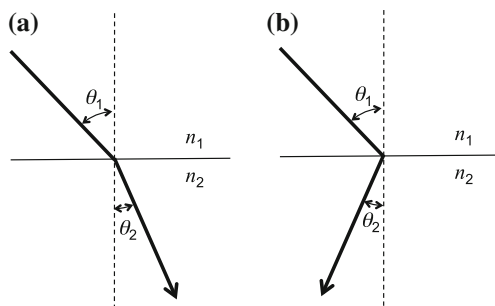
### 4.3 Negative Index Materials

One of the interesting optical properties of metamaterials is negative refractive index. Let us consider refraction at a boundary as shown in Fig. 4.4a. Light is incident to medium 2 from medium 1, whose refractive indexes are  $n_2$  and  $n_1$  respectively, at an angle of incidence  $\theta_1$ . The Snell's law gives the angle of refraction  $\theta_2$

$$n_1 \sin \theta_1 = n_2 \sin \theta_2. \quad (4.3)$$

This law is equivalent to conservation of in-plane component of wavevector across the boundary. For negative  $n_2$ , the angle of refraction  $\theta_2$  is negative, as shown in Fig. 4.4b. This phenomenon is different from diffraction. One may understand the difference when light is traveling in a NIM. Suppose that light is traveling the direction  $z$ . In a usual medium, the phase of light is proceeding to the same direction. However, in the case of NIM, the phase of light in the NIM proceeds in the opposite direction. This means that a more distant object looks closer. There are many other interesting phenomena observed in the NIM, exemplified by the inverse Doppler effect and inverse Cherenkov radiation.

**Fig. 4.4** Refraction at boundary. **a**  $n > 0$  and **b**  $n < 0$



In NIM, both permittivity and permeability are negative. To fabricate such medium, the control of permeability is necessary. Negative permittivity is rather easy, since existing matters such as metals have negative permittivity. In contrast, production of a medium with negative permeability is a thorny problem. At microwave or terahertz frequencies, this can be realized by using an array composed of ring resonators as shown in Fig. 4.3. The dimension of the resonators is in the order of micrometer or millimeters [7, 8]. However it is difficult to fabricate such ring resonators at optical frequencies because of the following two reasons: (a) it is too small and (b) losses in metals are remarkable at optical frequencies. A few structures are proposed instead of the use of the ring resonators. Metallic rod-pairs show negative index in the infrared frequency range [9] and nanometer fishnet structures show negative index at visible wavelengths [10, 11]. The latter structure can be extended to bulky NIM having a thickness. Later, bulky NIMs of a stack of fishnet structure is reported, [12] which work at a wavelength of  $1.5 \mu\text{m}$  and the refraction at negative angles is observed. The optical property appearing as a result of the control the permeability, other than NIM, is a Brewster angle for s-polarized light. This is theoretically predicted [13] and experimentally realized at a microwave frequency [14]

#### 4.4 Effective Medium Approximation

Metamaterials are composite medium composed of metallic nanostructures and matrix media such as air. To calculate the optical constants of metamaterials, such as refractive index and susceptibilities, the homogenization treatment is necessary. The effective medium approximation (EMA) is mostly used. There are four kinds of EMA methods: (a) the parallel capacitor model, (b) serial capacitor model, (c) Maxwell Garnett model and (d) Bruggeman's EMA. Let us consider a composite of two media 1 and 2 with permittivity  $\epsilon_1$  and  $\epsilon_2$ . Suppose the volume fraction  $f_1$  of medium 1. The models of the two-component composite are schematically illustrated in Fig. 4.5. The parallel capacitor model is the simplest approximation. The two media form capacitors, which form a parallel circuit. Then the effective permittivity  $\epsilon_{\text{eff}}$  is

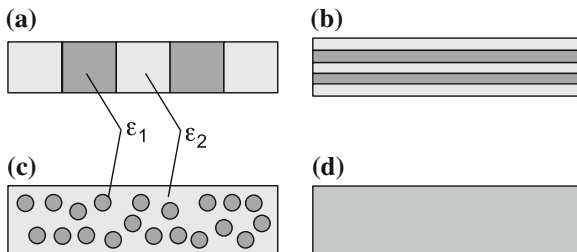


**Fig. 4.5** Schematics of (a) the parallel capacitor model, (b) serial capacitor model, (c) Maxwell Garnett model and (d) Bruggeman's EMA

described as

$$\epsilon_{\text{eff}} = f_1 \epsilon_1 + (1 - f_1) \epsilon_2. \tag{4.4}$$

In this model, it is assumed that no interaction exists between the two media. In contrast, the serial capacitor model considers strong interaction between the media. The capacitor from a serial circuit as described in (b). Then the effective permittivity  $\epsilon_{\text{eff}}$  is described as

$$\epsilon_{\text{eff}}^{-1} = f_1 \epsilon_1^{-1} + (1 - f_1) \epsilon_2^{-1}. \tag{4.5}$$

In the Maxwell Garnett model, it is assumed that spheres of medium 1 dispersed in medium 2. Then the effective permittivity  $\epsilon_{\text{eff}}$  is described as

$$\frac{\epsilon_{\text{eff}} - 1}{\epsilon_{\text{eff}} + 2} = f_1 \frac{\epsilon_1 - 1}{\epsilon_1 + 2} + (1 - f_1) \frac{\epsilon_2 - 1}{\epsilon_2 + 2}. \tag{4.6}$$

The Maxwell Garnett model is equivalent to the Claudius-Mosotti relation, used to relate the refractive index and molecular polarizability. The Bruggeman’s EMA is proposed as a result of development of the Maxwell Garnett model. In this model the effective permittivity  $\epsilon_{\text{eff}}$  is described as

$$f_1 \frac{\epsilon_1 - \epsilon_{\text{eff}}}{\epsilon_1 + 2\epsilon_{\text{eff}}} + (1 - f_1) \frac{\epsilon_2 - \epsilon_{\text{eff}}}{\epsilon_2 + 2\epsilon_{\text{eff}}} = 0. \tag{4.7}$$

Figure 4.6 summarizes the effective permittivity as a function of  $f_1$  using the four different EMAs. In (a), the calculation was made for a dielectric medium with permittivity  $\epsilon_1 = 2.5$  is dispersed in a medium 2 with  $\epsilon_2 = 1$ . In (b) it was made for a metallic medium  $\epsilon_1 = -3.17 + 3.11i$  (Au at 510nm) is dispersed in a medium 2 with  $\epsilon_2 = 1$ . The calculated results are very different in the case of (b). Although the

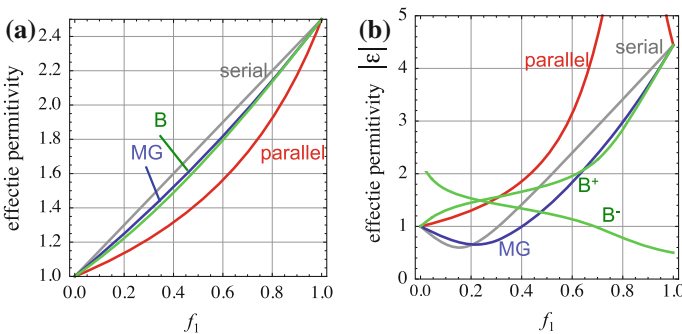


**Fig. 4.6**  $\epsilon_{\text{eff}}$  as a function of  $f_1$  using (i) the parallel capacitor model, (ii) serial capacitor model, (iii) Maxwell Garnett model (MG) and (iv) Bruggeman’s EMA (B). **a** A dielectric medium with permittivity  $\epsilon_1 = 2.5$  is dispersed in a medium 2 with  $\epsilon_2 = 1$ . **b** A metallic medium  $\epsilon_1 = -3.17 + 3.11i$  (Au at 510nm) is dispersed in a medium 2 with  $\epsilon_2 = 1$

Bruggeman’s EMA has two solutions  $B^+$  and  $B^-$  in (b),  $B^+$  is real. The application of EMA to metamaterials should be carefully.

### 4.5 Super Resolution

The super resolution, a resolution over diffraction limit (approximately a half wavelength of light), is one of important applications of NIM. Veselago proposed a perfect lens of NIM, which enables us the super resolution microscopy [2]. The lens is a thin slab of NIM with a refractive index of  $-1$ . This utilizes the fact that the angle of refraction is equal to angle of incidence with the opposite sign, as shown in Fig. 4.7. An image of the small object is formed on the other side of the super lens. In practice, however, this type of super resolution is difficult. The metamaterials cannot be regarded as a continuous medium because the resonance unit of the metamaterials is usually large in the order of 100 nm. Therefore no demonstration of the super resolution was made so far at optical frequencies.

Another super resolution is proposed by Pendry, [3] in which a metallic slab is used, as shown in Fig. 4.8. An object smaller than the wavelength of light forms an image adjacent to the metallic slab through evanescent wave and surface plasmons. Feng et al. demonstrated the super resolution that a chromium thin wire is imaged in a polymer photo-registration film through a 35 nm thick silver film [15]. The structure of the image was probed by atomic force microscope. In this case, the image is not magnified, so that we need to probe the image by the method other than the optical. Zhang et al. reported an optical setup to magnify the image [16]. The geometry is shown in Fig. 4.9. It was demonstrated that two lines separated by 150 nm was imaged using a conventional lens. The observation could be made with a CCD detector. In contrast to the scanning near-field optical microscopy, which also provides optical

**Fig. 4.7** Super resolution with a perfect lens of a NIM slab proposed by Veselago [2]

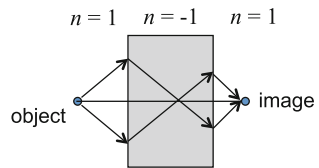


**Fig. 4.8** Plasmonic super resolution [13]

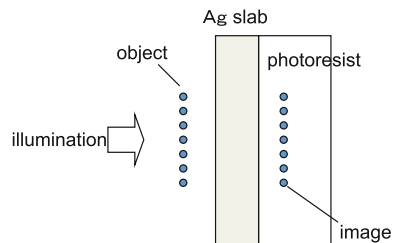
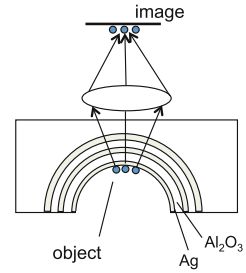


**Fig. 4.9** Super resolution with magnification [14]



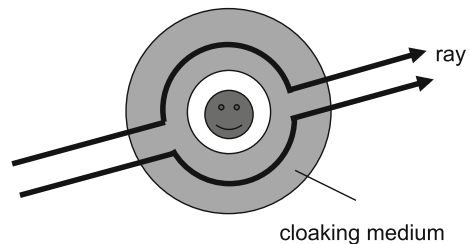
super resolution, we can observe the objects at a video rate. Optical microscopy can be made the objects in a liquid such as water. Hence it will be a powerful tool in biology.

## 4.6 Cloaking

Another interesting application of metamaterials is optical cloaking. Cloaking is a technique that makes an object invisible. One possible way is to cloak the object with a medium designed in such a way that the light detours the object, as shown in Fig. 4.10. Leonhardt proposed the spatial distribution of the refractive indexes in order to perform cloaking [17]. For this purpose, however, we need unrealistic range of refractive indexes from 0 to 36. Pendry and Smith proposed a cloaking using anisotropic metamaterials, and later they experimentally demonstrated the cloaking at the microwave frequencies [18, 19].

In the Pendry and Smith's proposal, the medium with  $\mu \neq 1$  is required. This is not convenient for cloaking at optical frequencies. Shalaev et al. proposed a structure for cloaking in which metallic nanorods are distributed whose long axis is aligned along the radial direction of a cylinder, as shown in Fig. 4.11 [20]. In this method, only spatial distribution of permittivity is required. The dielectric matrix has a positive permittivity, whereas the metallic nanorod has negative one. The effective permittivity of composite materials of the nanorod and dielectric matrix can be ranged from negative to positive by changing the density of the nanorods. They designed a cylindrical composite system working as a cloaking medium. The medium with

**Fig. 4.10** Cloaking a object





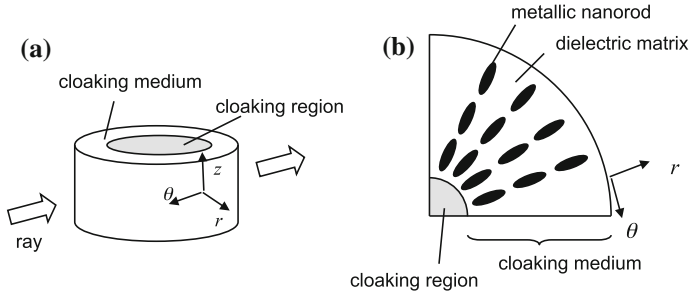


**Fig. 4.11** Cloaking with nonmagnetic ( $\mu = 1$ ) materials [20]

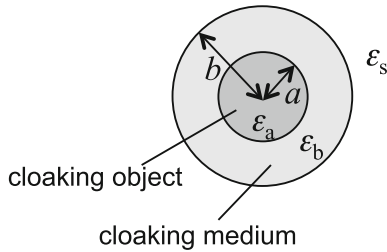


**Fig. 4.12** Cloaking by core-shell structure

the effective permittivity depends on the distance from the center, since the density of the nanorod decreases. The medium with the permittivity distribution works as a cloaking medium, according to their theoretical calculation. They demonstrated the cloaking behavior by numerical simulation.

A different approach to cloak an object is proposed by Alu and Engheta [21]. They use optical response of a core-shell structure. Suppose a system that a spherical cloaking object with a diameter  $a$  and permittivity  $\epsilon_a$  is surrounded by a shell with  $a$  thickness  $b$  and permittivity  $\epsilon_b$ , as shown in Fig. 4.12. When the core-shell particle is much smaller than the wavelength of light, the total polarizability  $\alpha$  can be described as [22]

$$\alpha = 4\pi b^3 \frac{(\epsilon_b - 2\epsilon_s)(\epsilon_a + 2\epsilon_b) + \left(\frac{a}{b}\right)^3 (\epsilon_a - \epsilon_b)(\epsilon_s + 2\epsilon_b)}{(\epsilon_b + 2\epsilon_s)(\epsilon_a + 2\epsilon_b) + 2\left(\frac{a}{b}\right)^3 (\epsilon_b - \epsilon_s)(\epsilon_a - \epsilon_b)} \quad (4.8)$$

where  $\epsilon_s$  is the permittivity of ambient medium. When the numerator of Eq. 4.8 is zero, the polarizability is absent. This means that the particle is invisible and the core is cloaked. They calculated and showed the possibility of the cloaking at visible wavelengths, if the shell is made of a medium with negligible loss. This method is not universal, but is a possible method to realize cloaking.

## References

1. V.M. Shalaev, Nat. Photonics **1**, 41 (2007)
2. F.G. Veselago, Sov. Phys. Usp **10**, 509 (1968)
3. J.B. Pendry, Phys. Rev. Lett. **85**, 3966 (2000)
4. R.A. Shelby, D.R. Smith, S. Schultz, Science **292**, 77 (2001)
5. M. Notomi, Phys. Rev. B **62**, 10696 (2000)
6. J.B. Pendry, A.J. Holden, D.J. Robbins, W.J. Stewart, IEEE Trans. Microw. Theory Tech. **47**, 2075 (1999)
7. T.J. Yen, W.J. Padilla, N. Fang, D.C. Vier, D.R. Smith, J.B. Pendry, D.N. Basov, X. Zhang, Science **303**, 1494 (2004)
8. S. Zhang, W. Fan, K.J. Malloy, S.R.J. Brueck, N.C. Panoiu, R.M. Osgood, J. Opt. Soc. Am. B **23**, 434 (2006)
9. V.M. Shalaev, W.C. Uday, K. Chettiar, H.-K. Yuan, A.K. Sarychev, V.P. Drachev, A.V. Kildishev, Opt. Lett. **30**, 3356 (2005)
10. G. Dolling, C. Enkrich, M. Wegener, C.M. Soukoulis, S. Linden, Opt. Lett. **32**, 53 (2007)
11. G. Dolling, M. Wegener, C.M. Soukoulis, S. Linden, Opt. Lett. **31**, 1800 (2006)
12. J. Valentine, S. Zhang, T. Zentgraf, E. Ulin-Avila, D.A. Genov, G. Bartal, X. Zhang, Nature **455**, 376 (2008)
13. T. Tanaka, A. Ishikawa, S. Kawata, Phys. Rev. B **73**, 125423 (2006)
14. Y. Tamayama, T. Nakanishi, K. Sugiyama, M. Kitano, Phys. Rev. B **73**, 193104 (2006)
15. N. Fang, H. Lee, C. Sun, X. Zhang, Science **308**, 534 (2005)
16. Z. Liu, H. Lee, Y. Xiong, C. Sun, X. Zhang, Science **315**, 1686 (2007)
17. U. Leonhardt, IEEE J. Sel. Top. Quantum Electron. **9**, 102 (2003)
18. J.B. Pendry, D. Schurig, D.R. Smith, Science **312**, 1780 (2006)
19. D. Schurig, J.J. Mock, B.J. Justice, S.A. Cummer, J.B. Pendry, A.F. Starr, D.R. Smith, Science **314**, 977 (2006)
20. W. Cai, U.K. Chettiar, A.V. Kildishev, V.M. Shalaev, Nat. Photonics **1**, 224 (2007)
21. A. Alu, N. Engheta, Phys. Rev. Lett. **100**, 113901 (2008)
22. C.F. Bohren, D.R. Huffman, *Absorption and Scattering of Light by Small Particles* (Wiley, New York, 1983), p. 149